# Analyst

Accepted Manuscript






ROYAL SOCIETY OF CHEMISTRY

www.rsc.org/analyst

# Isotope Labelling - Paired Homologous Double Neutral Loss Scan -Mass Spectrometry for Profiling of Metabolites with Carboxyl Group

Yun-Qing Huang,† Qiu-Yi Wang,† Jia-Qi Liu, Yan-Hong Hao, Bi-Feng Yuan, Yu-Qi Feng*

*These authors contributed equally to this work.*

*Key Laboratory of Analytical Chemistry for Biology and Medicine (Ministry of Education), Department of Chemistry, Wuhan University, Wuhan 430072, China*

***** Corresponding author. Tel.:+86-27-68755595; fax: +86-27-68755595.

***E-mail address:*** yqfeng@whu.edu.cn

## Abstract:

We developed a novel method for non-targeted screening of metabolites by high performance liquid chromatography - mass spectrometry with paired homologous double neutral loss scan mode after *in vitro* isotope labelling (IL-HPLC-PHDNL-MS). As a proof of concept, we investigated the carboxylic acid metabolites profiling in plant samples by the IL-HPLC-PHDNL-MS method. To this end, *N*,*N*-dimethylaminobutylamine (DMBA) and $d^4$-*N*,*N*-dimethylaminobutylamine ($d^4$-DMBA) were synthesized and utilized to label carboxylic acids. Our results show the MS response of carboxylic acids were enhanced by 20- to 40-fold after labelling. As for the IL-HPLC-PHDNL-MS analysis, DMBA and $d^4$-DMBA labelled samples were mixed equally before MS analysis. Because the isotope labelled moieties (dimethylamino moiety, $Me_2N$) of DMBA and $d^4$-DMBA are easily ruptured and lost as neutral fragments (NL 45 and NL 49) under collision induced dissociation (CID), two neutral loss scan can be carried out simultaneously to record the signals of DMBA and $d^4$-DMBA labelled samples, respectively. In this respect, the metabolites from two samples labelled with different isotope reagents are ionized at the same time but recorded separately by mass spectrometry, which can eliminate the MS response fluctuation and mutual interference. Using this method, six potential biomarkers involved in wound tomato leaves were identified, and their structures were further elucidated by product-ion scan and high resolution mass spectrometry analysis. Taken together, the IL-HPLC-PHDNL-MS method demonstrated good performance on the identification as well as relative quantification of metabolites with carboxyl group in biological samples.


**Keywords:** paired homologous double neutral loss scan; isotope labelling; mass spectrometry; carboxylic acid metabolites

## Introduction

Metabolomics aims at qualitative and quantitative analysis of all low-molecular-weight metabolites of a living cell, organ or whole organism.[1] With the rapid development of analytical methods, metabolomics has drawn much attention in disease diagnosis, nutrition science, and drug discovery.[2] Metabolomics is presented with the challenge of enormous chemical diversity of metabolites. To date, non-targeted analysis demonstrates to be an effective approach that has the advantages of probing the entire metabolic space and can be used to discover potential biomarkers.[3-5]

Mass spectrometry (MS) is one of the most prominent platforms for non-targeted metabolite profiling due to its great sensitivity and mass accuracy. Gas chromatography-mass spectrometry (GC-MS) was widely employed in the early stage of metabolomics studies.[6, 7] Later, the advent of electrospray ionization (ESI) has largely promoted the application of liquid chromatography-mass spectrometry (LC-MS) in the profiling of metabolites.[8-10] Whereas, there are still challenges in the quantitative profiling of metabolites using MS because the MS responses of metabolites fluctuate and ionization efficiencies alter even under the same liquid chromatography conditions. To correct the MS response variation, internal standard (s) was (were) added to biological samples before MS analysis, and the metabolite signals were normalized to those of the internal standards.[8-10] However, this strategy has some limitations. Firstly, the metabolites may not co-elute with the internal standards, therefore the effects of MS response fluctuation can't be fully eliminated. Secondly, it is difficult to determine the amounts of internal standards to add because the metabolites in biological samples are very diverse in structures and contents.

To circumvent these problems, *in vitro* isotope labelling strategy has been developed for non-targeted quantitative profiling of metabolites.[4, 5, 11-13]. This strategy, to some extent, derived from the *in vitro* chemical isotope labelling methods for quantitative proteomic analysis. The typical chemical isotope labelling methods include isotope-coded affinity tag (ICAT),[14, 15] stable isotope dimethyl labelling,[16, 17] tandem mass tags[18] and isobaric tags for relative and absolute quantification (iTRAQ).[19] However, the diversity and complexity of metabolites are much greater than proteins. In addition, the isotopic cluster peaks of unlabelled high abundance metabolites may overlap with the peaks of labelled metabolites existing in trace levels, which will increase the difficulty of spectra interpretation. Isotope labelling can also be achieved *in vivo*. Stable isotope labelling by amino acids in cell culture (SILAC)[20] and stable isotope labelling of mammals (SILAM)[21] have been invented and applied in quantitative proteomic analysis. Recently, a new *in vivo* isotope labelling method named isotopic ratio outlier analysis (IROA) has been invented and applied in metabolic analysis.[22, 23] Compared with the *in vitro* isotope labelling method, IROA is more comprehensive and has advantages of the removal of artifacts and the reinforced identification of target compounds. Despite IROA being more comprehensive, the protocol is relative complicated and mutual interference between differently labelled samples cannot be eliminated completely. Furthermore, systematic errors caused by biological isotopic effects may accumulate during cell growing.

In this respect, neutral loss (NL) scan which monitors the loss of a neutral fragment produced by the fragmentation of a precursor ion, can be a valuable alternative. This acquisition mode is very powerful for selective analysis of molecules that possess similar fragmentation pattern with at least one identical moiety. Compared to full scan method, neutral loss scan provides spectra with lower noise and

better detection sensitivity due to the good selectivity. For example, some low abundance biomarkers, which were originally buried in the background signals in the full scan method, can be successfully identified by neutral loss scan.[24-26] In addition, Jian et al.[27] have successfully developed a method for screening glutathione and cyanide adducts of metabolically activated drugs using neutral loss scan method. Similarly, Wagner et al.[28] have studied the neutral loss of thiol group for selective determination of mercapturic acids in urine samples. In addition, recent applications of HPLC-NL-MS have been employed in qualitative screening of glycosides[29-32] phosphopeptides[30] DNA adducts[33] lipids[34, 35] sulfonamides[3] and nitrated compounds[36] in biological samples. However, the neutral loss scan method limits in detecting a relatively narrow group of metabolites with at least an identical moiety.

Here, we developed a new method for non-targeted profiling of metabolites with an identical functional group by combining *in vitro* isotope labelling and neutral loss scan mass spectrometry analysis (Figure 1). Because the metabolisms of organic acids involved in wound healing of plant have been well studied,[37-39] we, as a proof of concept, focused on the study of carboxylic acid metabolites which have been reported to cover about sixty five percent of the metabolome.[11, 24] Like the conventional isotope labelling method, a pair of isotope labelling reagents (*N*,*N*-dimethylaminobutylamine, DMBA; $^{4}$d-*N*,*N*-dimethylaminobutylamine, d$^{4}$-DMBA) that contain reactive groups, isotopically labelled moieties and ionizable groups, was synthesized. The major advantage of the strategy is that the dimethylamino moieties of the labelling reagents used in this method were designed to be easily ruptured and lost as neutral fragment under collision induced dissociation (CID). In this regard, the heavy and light labelled metabolites shared the same chemical structures and daughter ions, but differ in both weights of quasi-molecular

ions and neutral loss fragments. Paired homologous neutral loss scan were performed simultaneously following HPLC separation. Thus, the heavy and light labelled metabolites were ionized at the same time but recorded separately by MS. The heavy and light labelled metabolites from two groups served as mutual internal standards to eliminate MS response fluctuation and matrix interference. Using this strategy, several potential biomarkers relative to the response to wound in tomato leaves were identified. And the structures of the identified potential biomarkers were further elucidated by product-ion scan and high resolution mass spectrometry analysis.

## Experimental Section

### Chemicals

Milli-Q water was used in preparation of all solutions. Benzoic anhydride, 1,4-diaminobutane, triethylamine, 2-chloro-1-methylpyridinium iodide (CMPI), $NaBH_3CN$ and chloroform were of analytical grade and purchased from Aladdin Reagent Co. (Shanghai, China). Formaldehyde (35% in water) and hydrochloric acid (37% in water) were purchased from Shanghai Chemical Reagent Co. (Shanghai, China). Deuterium formaldehyde ($d^4$-HCHO, 20% in water) was purchased from Sigma (St. Louis, MO, USA). Acetonitrile (HPLC grade) was obtained from Tedia Company (Fairfied, USA).

### Synthesis of the Derivatization Reagents

The pathway for the synthesis of *N*,*N*-dimethylaminobutylamine (DMBA) and $^4$d-*N*,*N*-dimethylaminobutylamine ($d^4$-DMBA) is shown in Figure S1. Briefly, 1,4-diaminobutane (50 mmol) and 100 mL $CHCl_3$ were added into a flask (250 mL). The mixture was saturated with high-purity nitrogen gas. Then benzoic anhydride (15 mmol) was added to the solution. The reaction was stirred and refluxed for 3 hours

followed by cooling to room temperature. The resulting solution was washed successively with water to remove unreacted 1,4-diaminobutane. Then the obtained solution was cooled in ice water bath. Formaldehyde (60 mmol) and $NaBH_3CN$ (60 mmol) were added to the above cooled solution successively while stirring vigorously. The reaction was continued for 15 minutes. After that, the reaction mixture was washed with saturated salt water (30 mL). The organic solvent was collected and dried over anhydrous magnesium sulfate ($MgSO_4$), and then removed by evaporating under reduced pressure below 35°C. The product was purified with a gel column with eluent containing methanol, ethyl acetate and triethylamine (1:10:0.1, v/v/v). The obtained pure product was hydrolyzed with concentrated hydrochloric acid by refluxing 48 hours. After cooling to room temperature, the mixture was extracted with ethyl acetate (50 mL × 3). The water solution was separated and dried by evaporating under reduced pressure. The obtained light yellow solid was dried in a vacuum desiccator over $P_2O_5$. DMBA, ESI-MS (*m/z*, 117), $^1$H NMR purity >95%; $^1$H NMR (DMSO-d6, 300 MHz), 1.58-1.82 (m, 4H), 2.70-2.75 (d, 6H), 2.76-2.83 (m, 2H), 3.02-3.07 (m, 2H), 8.31 (s, 3H), 10.8 (s, 1H). d$^4$-DMBA was prepared in a similar procedure with d$^4$-formaldehyde instead of formaldehyde. d$^4$-DMBA, ESI-MS (*m/z*, 121), $^1$H NMR purity >95%, $^1$H NMR (DMSO-d6, 300 MHz), 1.58-1.82 (m, 4H), 2.70-2.75 (d, 2H), 2.76-2.83 (m, 2H), 3.02-3.07 (m, 2H), 8.31 (s, 3H), 10.8 (s, 1H).

**General Procedure for the IL-HPLC-PHDNL-MS Analysis**

Tomato seeds from control group and wounded group were pretreated and labelled with DMAB and d$^4$-DMBA, respectively (Figure 1A). The heavy and light labelled samples were mixed with equal amount and then analyzed by HPLC-PHDNL-MS. The MS scan method consisted of two neutral loss scan corresponding to DMAB and d$^4$-DMBA labelled metabolites, respectively (Figure

1B). As for the reverse isotope labelling, the control group and wounded group were labelled with $d^4$-DMBA and DMAB, respectively. Metabolites with significant changes between control group and wounded group identified in both the forward and reverse isotope labelling modes were selected, and then further explored by product-ion scan and high resolution mass spectrometry analysis.

**Sample Preparation**

Tomato (*Lycopersicon esculentum* cv. Castlemart) was grown in peat pots and maintained under a day-night cycle of 16 h under light (30 $\mu E \cdot m^{-2} \cdot s^{-1}$) at 30°C and 8 h of darkness at 25°C. The tomato leaves were harvested 3 weeks later. For the preparation of wounded samples, all the leaves were crushed two to three times across the main vein with a hemostat as described in the literature.[40] After treatments, the tomato leaves were incubated under constant light for 15 minutes. Then all the wounded leaves of a tomato seedling were cut off. The cut leaves of three tomato leaves were combined, weighed and frozen in liquid nitrogen as soon as possible. The leaves of the control group were harvested simultaneously without crushing.

The extraction of the metabolites in tomato leaves were performed according to the previously described procedure.[41] Briefly, a packet of tomato leaves from three tomato leaves was ground into fine powder in liquid nitrogen. 100 mg of the powder was then extracted with a mixture solution of isopropanol, water and concentrated hydrochloric acid (100:50:0.1, v/v/v) in ice water bath while stirring for 30 minutes (1.0 mL per 100 mg fresh weigh of leaves). The obtained solution was further extracted with dichloromethane (2.0 mL per 100 mg fresh weigh of leaves) followed by drying under nitrogen gas.

Isotopic labelling of carboxylic metabolites from control and wounded group was performed subsequently. Shown in Figure S2 are the reactions of DMBA and

d$^4$-DMBA with carboxylic acid metabolites. Briefly, 400 µL acetonitrile, 20 µL CMPI (20 µmol/mL) and 30 µL triethylamine (20 µmol/mL) was added to the dried samples and then mixed by vortex. The mixture was then incubated at 40°C for 5 minutes. Then 40 µL DMBA (20 µmol/mL) or d$^4$-DMBA (20 µmol/mL) was added. The derivatization reaction was performed by keeping the mixture at 40°C for 60 minutes. The resulting solution was then dried under nitrogen gas and redissolved in 100 µL acetonitrile/water (1:10, v/v). Then the heavy labelled and light labelled sample solutions were mixed equally, and 50 µL of the solution was used for analysis by HPLC-PHDNL-MS system.

**HPLC-PHDNL-MS Analysis**

Analysis of samples was performed on the HPLC-ESI-MS/MS system consisting of an AB 3200 QTRAP LC-MS/MS (Applied Biosystems, Foster City, CA, USA) with an electrospray ionization source (Turbo Ionspray) and a Shimadzu LC-20AD HPLC (Tokyo, Japan) with two LC-20AD pumps, a SIL-20A auto sampler, a CTO-20AC thermostated column compartment and a DGU-20A3 degasser. The experiments were performed in either negative or positive ion mode. Data acquisition and processing were performed using AB SCIEX Analyst 1.5 Software (Applied Biosystems, Foster City, CA, USA). The HPLC separation was performed on a Shimadzu C-18 column (150×2.1 mm, 3 µm, Kyoto, Japan) with a flow rate of 0.2 mL/min at 35$^o$C. Formic acid in water (0.05%, v/v, solvent A) and a mixture of 0.05% formic acid in acetonitrile (v/v, solvent B) were employed as mobile phase. A gradient of 0 - 40 min from 10% B to 100% B, 40 - 45 min 100% B, 45 - 47 min from 100% B to 10% B, and 47 – 60 min 10% B was used.

The PHDNL scan method consists of two neutral loss scans (NL of 45 and 49 Da) in the range of *m/z* 200-600. PHDNL survey scan was performed on triple quadrupole

scan mode of AB 3200 QTRAP mass spectrometer. A full scan survey was performed in the same *m/z* range for comparison. The source and gas settings for both PHDNL and full scans were identical. PHDNL scan and full scan were carried out in the positive ion mode using a TurboIonSpray source (ESI). Source voltage was set at -4.8 kV and vaporizer temperature was set at 500°C. The mass spectrometer was operated with gas settings of 45 psi for turbogas, 30 psi for nebulizer gas, 30 psi for curtain gas, and 10 psi for collision gas. Scan time per cycle was 2.0 s with a pause of 5.0 ms for each scan. Resolution of Q1 and Q3 was set to "unit". Declustering potential, entrance potential, cell entrance potential, collision energy and cell exit potential were set at 40 V, 6 V, 8 V, 30 V and 4.5 V, respectively.

For structural identification, IDA (Information Dependent Acquisition) criteria were set as that EPI (Enhanced Product Ion Scan) was triggered when signals of the pre-selected metabolites by DNL scan exceeding 1,000 counts/s at their retention times. The mass tolerance was set to 250 mamu, and retention time tolerance was set to 30 s. EPIs were performed with different CEs (20, 35 and 50 V). Fragments formed in the EPI scans were detected in the range of *m/z* 50 to *m/z* 600 using dynamic fill and a scan rate of 5,000 amu/s.

High resolution mass spectrometry experiments were performed on a quadrupole-time of flight (qTOF, Agilent 6510, Agilent, J&W, Santa Clara, CA) mass spectrometer under positive mode in the range of *m/z* 100 to *m/z* 1000. Capillary voltage was set at 3.5 kV, skimmer voltage at 65 V, drying gas at 9 L/min, drying gas temperature at 350°C, nebulizer gas at 45 psi and scan speed at 2 spectra/s. Mass accuracy was 4 ppm and resolution was 10000 (FWHM) under their experimental conditions.

**Data Analysis**

Peak alignment and peak filtering were carried out with MarkerView software 1.0 (Applied Biosystems, Foster City, CA, USA). PHDNL data were processed using this software with the following parameters: minimum retention time, 2.0 min; maximum retention time, 60 min; noise threshold, 500 counts/s; minimum spectral peak width, 0.2 amu; minimum retention time peak width, 3 scans; maximum retention time peak width, 80 scans; retention time tolerance, 1.0 min; mass tolerance, 0.3 amu; maximum number of peaks, 500. The resulting aligned peak lists of the two neutral loss scans were then exported to Excel 2003 for comparison based on peak areas of the same metabolites which were differentially labelled. Metabolites with peak area ratios (wounded group / control group) greater than 1.50 or less than 0.667 were selected for further structure elucidation.

An integrated statistical analysis was performed using the SPSS 16.0 software package (Chicago, USA) that not only took into consideration fold differences in metabolite levels, but also calculated a statistical significance (*t*-test, $p < 0.01$) for ratios from six independent, biologically replicated experiments (3 for forward labelling, the other 3 for reverse labelling). Differences were considered significant when fold change >1.50 ($|\log_2(\text{fold change})|>0.585$), both up- and down-regulated, and $p < 0.01$ ($-\log_{10} p >2$).

## Results and Discussion

### Enhancement of Detection Sensitivity upon Derivatization

The carboxylic acid metabolites naturally occurring in biological samples can be ionized by ESI-MS under negative mode. But the ionization efficiency and detection sensitivity are relatively poor. To improve the intensities of ion signal, a tertiary amino group were incorporated into the carboxylic acid metabolites by derivatization

with DMBA. We analyzed the unlabelled mixture of gibberellic acid (GA3, 1.0 nmol/mL), jasmonic acid (JA, 1.0 nmol/mL) and dodecanoic acid (12-C fatty acid, 1.0 nmol/mL) by direct infusion in negative ion mode as well as the labelled mixture with the same concentration in positive ion mode under their own optimized MS conditions. The results showed that ESI-MS signals of DMBA labelled carboxylic acids increased by 20- , 25- and 40-fold for GA3, JA and 12-C fatty acid, respectively, which suggests that DMBA derivatization can remarkably improve the detection sensitivity of carboxylic acid metabolites (Figure 2).

**Fragmentation Behavior of DMBA Labelled Carboxylic Compounds**

To investigate the fragmentation behaviour of DMBA labelled carboxylic compounds, three carboxylic acids with different structures (JA, GA3 and 12-C fatty acid) were used. As for amide, theoretical study indicated that the amide nitrogen is not the thermodynamically favoured site of protonation in gas phase.[42] But proton transfer from carbonyl group or amino group to the amide nitrogen atom just needs to pass over a relative low energy barrier.[43] And protonation at the amide nitrogen atom destroys the *n*–p conjugation and makes the amide C–N bond facile to rupture. Therefore, the charge induced dissociation of amide is often observed in amide C–N bond. However, our results show that the fragmentation of DMBA derivatized carboxylic acids mainly occurred in the amine C–N bond, and the product ions generated from elimination of dimethylamine neutral fragment (NL 45) were the dominant products at low collision energy (25 V) (Figure 3).

Fragmentation via an intermediate ion - neutral complex provides a multistage pathway with a relatively low energy barrier, which has been found to be prevalent for many organic ions in the gas phase in the past decades. We reason that the fragmentation of DMBA labelled carboxylic acids proceeds via an intermediate of ion

- neutral complex generated from a neighbouring group participating rearrangement. The detailed fragmentation pathway of DMAB labelled 12-C fatty acid is shown in Figure 4. Briefly, lone pair electrons located at amide nitrogen atom attacks the carbon atom adjacent to the protonated dimethylamino group, thus, an ion-neutral complex comprising neutral dimethylamine and a cycled positive ion is formed. Rupture of the ion-neutral complex results in an intensive cycled positive ion (*m/z* 254) and a neutral fragment of dimethylamine (*m/z* 45). Intra-complex proton transfer was also found to result in the generation of protonated dimethylamine (*m/z* 46). The cycled positive ion (*m/z* 254) can be further dissociated through an intermediate of ion - neutral complex, which produces protonated pyrrolidine (*m/z* 72) and acylium positive ion (*m/z* 183). And mass peaks of product ions (*m/z* 100) are from loss of an alkene neutral fragment from the cycled positive ion (*m/z* 254). In addition, the ion of *m/z* 72 may be further dissociated in the ion trap. We found that the $MS^3$ spectrum of the ion of *m/z* 72 is similar with $MS^2$ spectrum of protonated pyrrolidine standard, confirming that neighbouring group participation plays an important role in the fragmentation of protonated amides.

The loss of neutral fragments $CO_2$ and $H_2O$ from some carboxylic acids under CID has been frequently observed before, which, however, is strongly dependent on the molecular structure and the fragmentations of different carboxylic acids can exhibit different behaviour.[25] This phenomenon is an obstacle for profiling of carboxylic acid metabolites by neutral loss scan. To circumvent this problem, we incorporated a moiety ($Me_2N$), which can be easily lost as a neutral fragment in collision cell, into carboxylic acid metabolites through DMBA labelling. As a result, the derivatization method makes it possible to screen carboxylic metabolites without bias.

## Quantitative Analysis

Mixture solutions of JA, GA3 and 12-C fatty acid were used to evaluate the quantitative analysis. One mixture solution at a concentration of 50 ng/mL for each analyte was labelled with $d^4$-DMAB. And the other mixture solutions with the same concentrations of JA, GA3 and 12-C fatty acid ranging from 5 ng/mL to 500 ng/mL were labelled with DMBA. Then the $d^4$-DMAB labelled mixture solution was mixed with each of DMAB labelled mixture solution (1:1, v/v) and analyzed by HPLC-PHDNL-MS. The regression curves were constructed by plotting mean peak area ratios of heavy/light versus the mean molar ratios of heavy/light based on data obtained from triplicate measurements. The results show that the slopes of regression lines of JA, GA3 and 12-C fatty acid were approximate to 1.00 (Table S1), indicating that the ratios of the chromatographic peak areas closely matched with the ratios of the different isotopes labelled analytes. The correlation coefficients ($R^2$) were also found to be close to 1.00, demonstrating a high correlation between the experimental and theoretical data. The relative standard deviations (RSDs) were less than 7.5%, suggesting a good precision of this method. In addition, the detection limits (LODs) for labeled JA, GA3 and 12-C fatty acid were 0.120, 0.252 and 0.0812 ng / mL, respectively.

## Analysis of Plant Samples and Data Mining

Using our proposed HPLC-PHDNL-MS strategy, we detected 103 metabolites in tomato leaves (two of them were detected only in wounded tomato leaves, Table S2). The relative standard deviations of absolute peak areas and peak area ratios are in the range of 13%-22% and 3.0%-8.0%, respectively, which indicates good precision in measuring fold-changes between wounded and non-wounded groups.

One-sample *t*-test was performed to examine the statistical significance of fold changes from six independently biological experiments (3 for forward labelling, the other 3 for reverse labelling). The statistics for the test are shown in Table S3, including *p*-values and 95% confidence interval estimates. The fold changes (both up- and down-regulated) larger than 1.50 and the *p*-values less than 0.01 were considered statistically significant difference. Figure 5 shows a volcano plot, where, for each of the 101 metabolites, $-\log_{10}$ (*p*-value of wounded vs non-wounded) is plotted against its corresponding $\log_2$ (fold change of wounded/non-wounded). The probe sets that meet our arbitrary criteria are shown as red filled squares. As indicated in the plot, the fold changes of four metabolites showed statistically significant difference upon wounded treatment. Taken together, totally six metabolites were found to change significantly in content between the wounded tomato leaves and untreated tomato leaves, and two of them were detected only in wounded tomato leaves (Table 1).

**Biological Interpretation of the Potential Biomarkers**

The structures of the six potential biomarkers were further explored by product ion scan and high resolution mass spectrometry analysis. The product ion mass spectra of the six potential biomarkers under three different collision energies (20V, 35V and 50V) are shown in Figure S3, S5, S7, S9, S11 and S13, respectively. The proposed fragmentation pathways are shown in Figure S4, S6, S8, S10, S12 and S14, respectively. We also searched the database of metabolomics (PlantCyc、METLIN and KEGG) for further confirmation of the identities of the potential biomarkers and investigation of their biological functions. Among the six metabolites, four metabolites are up-regulated in wounded tomato leaves, and the other two were only detected in wounded tomato leaves. Generally, the six potential biomarkers mainly involve in *β*-oxidation of fatty acids, degradation of ascorbic acid, and plant growth

regulators exhibiting resistance activity to wound stress. An integrative view plot of the metabolite changes for the wound stress of tomato leaves is shown in Figure 6.

Acyl-CoA (acyl-Coenzyme A) is the chemical intermediate in the *β*-oxidation of fatty acid metabolic pathway. *β*-oxidation fatty acid is the hydrolysis product of *β*-oxo-acyl-CoA by acyl-CoA thioesterase.[44, 45] In the current study, two *β*-oxidation fatty acids, 4-hydroxy-3-oxobutanoic acid and 3-oxo-nonanoic acid, are significantly up-regulated (Table 1), indicating the metabolic pathway of *β*-oxidation of fatty acid was enhanced in response to wound stress. Previously report showed that the metabolic pathway of *β*-oxidation of fatty acid induces reactive oxygen species,[46-48] which plays key roles in response to environmental stresses such as wound attacked by herbivorous animals.[49] The biosynthesis of signal molecules are activated immediately after the burst of reactive oxygen species for acquiring resistance against stress.[50] In our current study, it was found that the wound accelerated the metabolic pathway of *β*-oxidation of fatty acid and therefore induced more reactive oxygen species against stress.

Asparagusic acid, a plant growth inhibitor comparable to abscisic acid, was also proposed to strengthen plant resistance to stress.[51, 52] Our results show that asparagusic acid increased by 3.1 - fold in wounded tomato leaves (Table 1), which is consistent with previously reported function of asparagusic acid on the protection of plant upon wound. Furthermore, the burst of reactive oxygen species is also accompanied by up-regulation of enzymes participating in the biosynthesis of coumarin,[53-56] which has been found to involve in the defense response of plant cells.[57] In the current study, the increased 2,4-dihydroxycinnamate content (an intermediate in the biosynthesis pathway of coumarin) may enhance the biosynthesis of coumarin for the sake of defense to wound stress.

Reactive oxygen species benefit the protection of plant from environmental stress, whereas they also display disadvantageous aspects for living cells, such as oxidation of lipids. Nevertheless, several biological pathways, such as glutathione pathway, carotene pathway and vitamins C/E pathway, have been found to prevent damage of lipid peroxide.[50, 58] Vitamins C and E can co-ordinate in removing the endogenous free radicals. Lipid soluble vitamin E has the ability to sequester the lipid peroxide in cell membranes, while water soluble vitamin C regenerates oxidized vitamin E back to the active state (Figure 6). In the current study, we found a degradation product of vitamin C (L-threo-tetruronate) increased in the wounded tomato leaves. We supposed that the oxidization and then degradation of vitamin C is a response to the increased reactive oxygen species induced by wound.

**Comparison of Neutral Loss Scan and Full Scan Method**

The DMBA labelled wounded tomato sample was analyzed by LC-ESI-MS in both neutral loss scan (NL 45) and full scan mode under the same chromatography condition. Figure 7A shows the full scan mass spectrum at the retention time of 3-oxo-nonanoic acid (18.6-19.2 min, *m/z* 271), which was buried in noise signals. Nevertheless, the mass spectrum obtained in neutral loss scan mode at the same retention time is much more clear (Figure 7B). The distinctly identified quasi-molecular ions of the metabolites are beneficial for the further interrogation of their structures.

## Conclusion

We developed an IL-HPLC-PHDNL-MS method using a pair of newly designed and synthesized isotope labelling reagent for non-targeted study of carboxylic metabolites. The method significantly improved the ionization efficiency of

carboxylic metabolites (20-40 folds increase), selectivity and quantification reproducibility. Using this method, we identified six potential biomarkers relevant to wound stress in tomato leaves. The six potential biomarkers mainly involved in $\beta$-oxidation of fatty acids, degradation of ascorbic acid, and plant growth regulators exhibiting resistance activity to wound stress. Moreover, the method can extend the application of neutral loss scan to the efficient identification of a relative wide group of metabolites with an identical functional group.

## Acknowledgements

The authors thank the financial support from the National Basic Research Program of China (973 Program) (2013CB910702, 2012CB720601), the National Natural Science Foundation of China (91217309, 91017013, 21205091, 21228501), the Fundamental Research Funds for the Central Universities.

## References

1. S. Moco, J. Vervoort, R. J. Bino, R. C. H. De Vos and R. Bino, *TrAC Trends in Analytical Chemistry*, 2007, **26**, 855-866.
2. R. Wei, *Curr Drug Metab*, 2011, **12**, 345-358.
3. C. Huang, B. Guo, X. Wang, J. Li, W. Zhu, B. Chen, S. Ouyang and S. Yao, *Analytica Chimica Acta*, 2012, **737**, 83-98.
4. H. M. Chapman, K. L. Schutt, E. M. Dieter and S. M. Lamos, *Bioanalysis*, 2012, **4**, 2525-2541.
5. R. C. H. De Vos, S. Moco, A. Lommen, J. J. B. Keurentjes, R. J. Bino and R. D. Hall, *Nat. Protocols*, 2007, **2**, 778-791.
6. M. M. Koek, R. H. Jellema, J. van der Greef, A. C. Tas and T. Hankemeier, *Metabolomics*, 2011, **7**, 307-328.
7. Z. T. Lei, D. V. Huhman and L. W. Sumner, *Journal of Biological Chemistry*, 2011, **286**, 25435-25442.
8. D. Rojo, C. Barbas and F. J. Ruperez, *Bioanalysis*, 2012, **4**, 1235-1243.
9. B. Guo, B. Chen, A. M. Liu, W. T. Zhu and S. Z. Yao, *Current Drug Metabolism*, 2012, **13**, 1226-1243.
10. S. Becker, L. Kortz, C. Helmschrodt, J. Thiery and U. Ceglarek, *Journal of Chromatography B-Analytical Technologies in the Biomedical and Life Sciences*, 2012, **883**, 68-75.

11. K. Guo and L. Li, *Analytical Chemistry*, 2010, **82**, 8789-8793.
12. X. Huang and F. E. Regnier, *Analytical Chemistry*, 2007, **80**, 107-114.
13. C. Bueschl, R. Krska, B. Kluger and R. Schuhmacher, *Anal Bioanal Chem*, 2013, **405**, 27-33.
14. K. C. Hansen, G. Schmitt-Ulms, R. J. Chalkley, J. Hirsch, M. A. Baldwin and A. Burlingame, *Mol. Cell Proteomics*, 2003, **2**, 299-314.
15. S. P. Gygi, B. Rist, S. A. Gerber, F. Turecek, M. H. Gelb and R. Aebersold, *Nat. Biotechnol.*, 1999, **17**, 994-999.
16. P. J. Boersema, R. Raijmakers, S. Lemeer, S. Mohammed and A. J. Heck, *Nat. Protoc.*, 2009, **4**, 484-494.
17. J.-L. Hsu, S.-Y. Huang, N.-H. Chow and S.-H. Chen, *Anal. Chem.*, 2003, **75**, 6843-6852.
18. A. Thompson, J. Schäfer, K. Kuhn, S. Kienle, J. Schwarz, G. Schmidt, T. Neumann and C. Hamon, *Anal. Chem.*, 2003, **75**, 1895-1904.
19. P. L. Ross, Y. N. Huang, J. N. Marchese, B. Williamson, K. Parker, S. Hattan, N. Khainovski, S. Pillai, S. Dey and S. Daniels, *Mol. Cell Proteomics*, 2004, **3**, 1154-1169.
20. S.-E. Ong, B. Blagoev, I. Kratchmarova, D. B. Kristensen, H. Steen, A. Pandey and M. Mann, *Mol. Cell Proteomics*, 2002, **1**, 376-386.
21. N. Rauniyar, D. B. McClatchy and J. R. Yates Iii, *Methods*, 2013, **61**, 260-268.
22. G. S. Stupp, C. S. Clendinen, R. Ajredini, M. A. Szewc, T. Garrett, R. F. Menger, R. A. Yost, C. Beecher and A. S. Edison, *Anal. Chem.*, 2013, **85**, 11858-11865.
23. F. A. de Jong and C. Beecher, *Bioanalysis*, 2012, **4**, 2303-2314.
24. R. J. C. A. Steen, I. Bobeldijk and U. A. T. Brinkman, *Journal of Chromatography A*, 2001, **915**, 129-137.
25. J. Dron, G. Eyglunent, B. Temime-Roussel, N. Marchand and H. Wortham, *Analytica chimica acta*, 2007, **605**, 61-69.
26. J. Qu, Q. Liang, G. Luo and Y. Wang, *Analytical Chemistry*, 2004, **76**, 2239-2247.
27. W. Y. Jian, H. F. Liu, W. P. Zhao, E. Jones and M. S. Zhu, *Journal of the American Society for Mass Spectrometry*, 2012, **23**, 964-976.
28. S. Wagner, K. Scholz, M. Donegan, L. Burton, J. Wingate and W. Volkel, *Analytical Chemistry*, 2006, **78**, 1296-1305.
29. S. Kazuno, M. Yanagida, N. Shindo and K. Murayama, *Analytical biochemistry*, 2005, **347**, 182-192.
30. H. H. Hsiao and H. Urlaub, *Proteomics*, 2010, **10**, 3916-3921.
31. F. Teichert, S. Winkler, H. C. Keun, W. P. Steward, A. J. Gescher, P. B. Farmer and R. Singh, *Rapid Communications in Mass Spectrometry*, 2011, **25**, 2071-2082.
32. J. Qu, Q. L. Liang, G. Luo and Y. M. Wang, *Analytical Chemistry*, 2004, **76**, 2239-2247.

33. D. Compagnone, R. Curini, G. D'Ascenzo, M. Del Carlo, C. Montesano, S. Napoletano and M. Sergi, *Analytical and Bioanalytical Chemistry*, 2011, **401**, 1983-1991.
34. T. A. Lydic, J. V. Busik, W. J. Esselman and G. E. Reid, *Analytical and Bioanalytical Chemistry*, 2009, **394**, 267-275.
35. D. Schwudke, J. Oegema, L. Burton, E. Entchev, J. T. Hannich, C. S. Ejsing, T. Kurzchalia and A. Shevchenko, *Analytical Chemistry*, 2006, **78**, 585-595.
36. T. T. J. Williams and H. Perreault, *Rapid Communications in Mass Spectrometry*, 2000, **14**, 1474-1481.
37. M. A. Noordermeer, G. A. Veldink and J. F. Vliegenthart, *Chembiochem*, 2001, **2**, 494-504.
38. A. Conconi, M. Miquel and C. Ryan, *Plant Physiology*, 1996, **111**, 797-803.
39. A. Kessler and I. T. Baldwin, *Annu. Rev. Plant Biol.*, 2002, **53**, 299-328.
40. L. Li, C. Li, G. Lee and G. Howe, *PNAS*, 2002, **99**, 6416.
41. X. Pan, R. Welti and X. Wang, *Nat. Protocols*, 2010, **5**, 986-992.
42. C. L. Perrin, *Acc. Chem. Res.*, 1989, **22**, 268-275.
43. Y.-P. Tu and A. G. Harrison, *J. Am. Soc. Mass. Spectrom.*, 1998, **9**, 454-462.
44. M. C. Hunt and S. E. H. Alexson, *Progress in Lipid Research*, 2002, **41**, 99-130.
45. C. Dellomonaco, J. M. Clomburg, E. N. Miller and R. Gonzalez, *Nature*, 2011, **476**, 355-359.
46. F. J. Corpas, J. B. Barroso and L. A. del Río, *Trends in Plant Science*, 2001, **6**, 145-150.
47. R. Mittler, *Trends in Plant Science*, 2002, **7**, 405-410.
48. A. Baker, I. A. Graham, M. Holdsworth, S. M. Smith and F. L. Theodoulou, *Trends in Plant Science*, 2006, **11**, 124-132.
49. J. J. Grant and G. J. Loake, *Science Signaling*, 2000, **124**, 21.
50. W. Durrant and X. Dong, *Annu. Rev. Phytopathol.*, 2004, **42**, 185-209.
51. R. J. Parry, A. E. Mizusawa, I. C. Chiu, M. V. Naidu and M. Ricciardone, *Journal of the American Chemical Society*, 1985, **107**, 2512-2521.
52. Y. Kitahara, H. Yanagawa, T. Kato and N. Takahashi, *Plant and Cell Physiology*, 1972, **13**, 923-925.
53. V. A. Katz, O. U. Thulke and U. Conrath, *Plant Physiology*, 1998, **117**, 1333-1339.
54. H. Kauss, E. Theisinger ‐ Hinkel, R. Mindermann and U. Conrath, *The Plant Journal*, 1992, **2**, 655-660.
55. H. Kauss, R. Franke, K. Krause, U. Conrath, W. Jeblick, B. Grimmig and U. Matern, *Plant Physiology*, 1993, **102**, 459-466.
56. O. Thulke and U. Conrath, *The Plant Journal*, 1998, **14**, 35-42.
57. U. Matern, *Planta Medica*, 1991, **57**, S15-S20.
58. G. Noctor, *Plant, Cell & Environment*, 2006, **29**, 409-425.

**Table 1.** The information of the identified six metabolites showing significant difference of content between wounded tomato leaves and untreated tomato leaves. The analytes were examined by high resolution mass spectrometry. Peak area ratios (wounded / untreated) were based on triplicate measurements.

| RT[a]/ min | *m/z* [b] | M1 [c] | M2 [d] | Formula | Structure | W/N [e] |
|---|---|---|---|---|---|---|
| 2.6 | 217.1586 | 118.0305 | 118.0266 | $C_4H_6O_4$ | 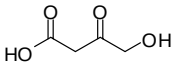 4-hydroxy-3-oxobutanoic acid | Only detected in wounded group |
| 2.5 | 233.1540 | 134.0259 | 134.0215 | $C_4H_6O_5$ | 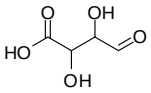 L-threo-tetruronate | 1.54 |
| 13.6 | 249.1066 | 149.9885 | 149.9809 | $C_4H_6O_2S_2$ | 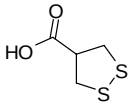 Asparagusic acid | 2.86 |
| 4.7 | 254.1535 | 155.0254 | 155.0218 | $C_6H_5NO_4$ | 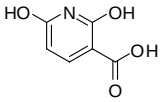 2,6-Dihydroxynicotinate | 2.16 |
| 18.7 | 271.2462 | 172.1281 | 172.1099 | $C_9H_{16}O_3$ | 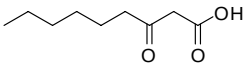 3-oxo-nonanoic acid | 4.01 |
| 6.6 | 279.1756 | 180.0475 | 180.0422 | $C_9H_8O_4$ | 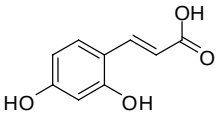 2,4-dihydroxycinnamate | Only detected in wounded group |

[a] Retention time.

[b] *m/z* of the labelled metabolites measured by high resolution mass spectrometry.

[c] Calculated *m/z* of the unlabelled metabolites according to *m/z* of labelled metabolites measured by high resolution mass spectrometry.

[d] Theoretical *m/z* of the unlabelled metabolites.

[e] Peak area ratios of wounded / untreated.

## Figure legends

**Figure 1**. (A) Reaction between DMBA and carboxylic acid compounds. (B) Schematic diagram of the principle of IL-HPLC-PHDNL-MS.

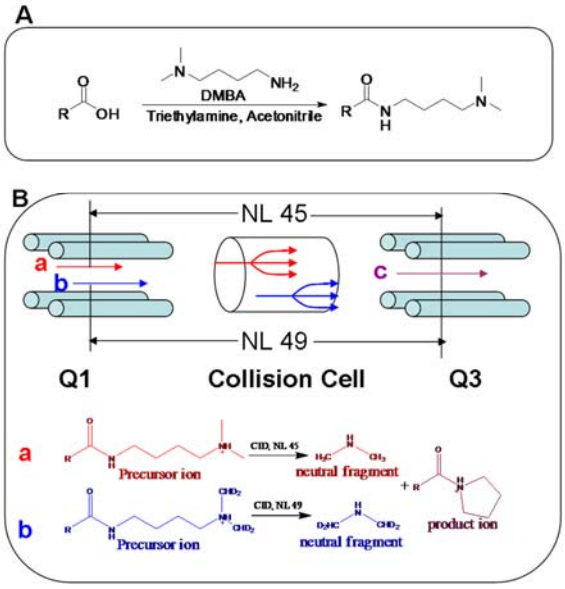

**Figure 2**. Comparison of ion signals between labelled (A) and unlabelled analytes (B) under their own optimized MS conditions. All the concentrations of GA3, JA and 12-C fatty acid were 1.0 nmol/mL. Labelled GA3, *m/z* 431; labelled JA, *m/z* 309; labelled 12-C fatty acid, *m/z* 299. Unlabelled GA3, *m/z* 331; unlabelled JA, *m/z* 209; unlabelled 12-C fatty acid, *m/z* 199.

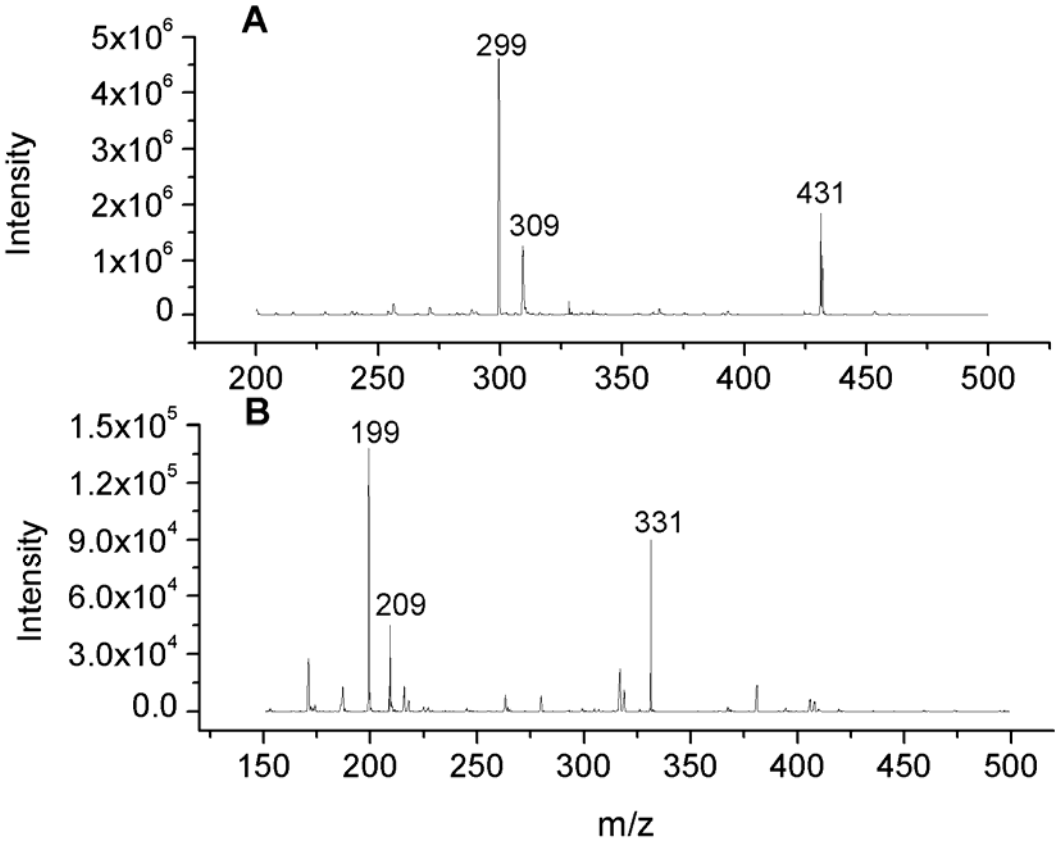

**Figure 3** The product ion mass spectra of DMBA labelled JA, GA3 and 12-C fatty acid.

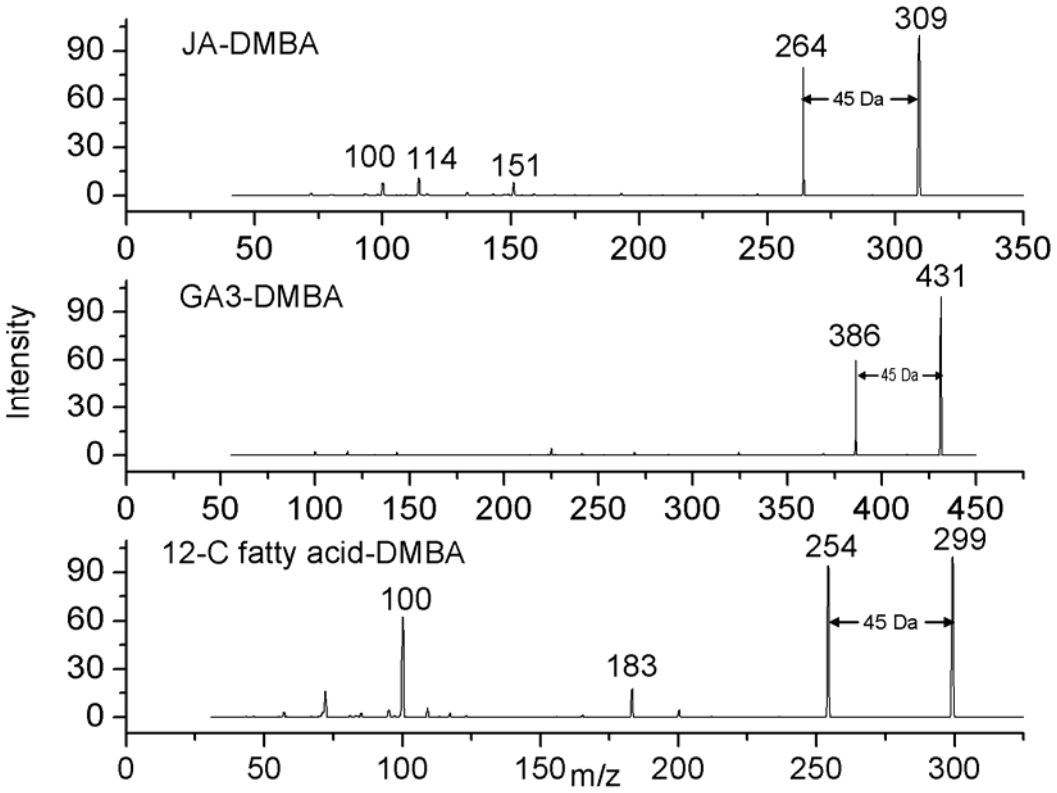

**Figure 4** The proposed fragmentation pathway of DMAB labelled 12-C fatty acid.

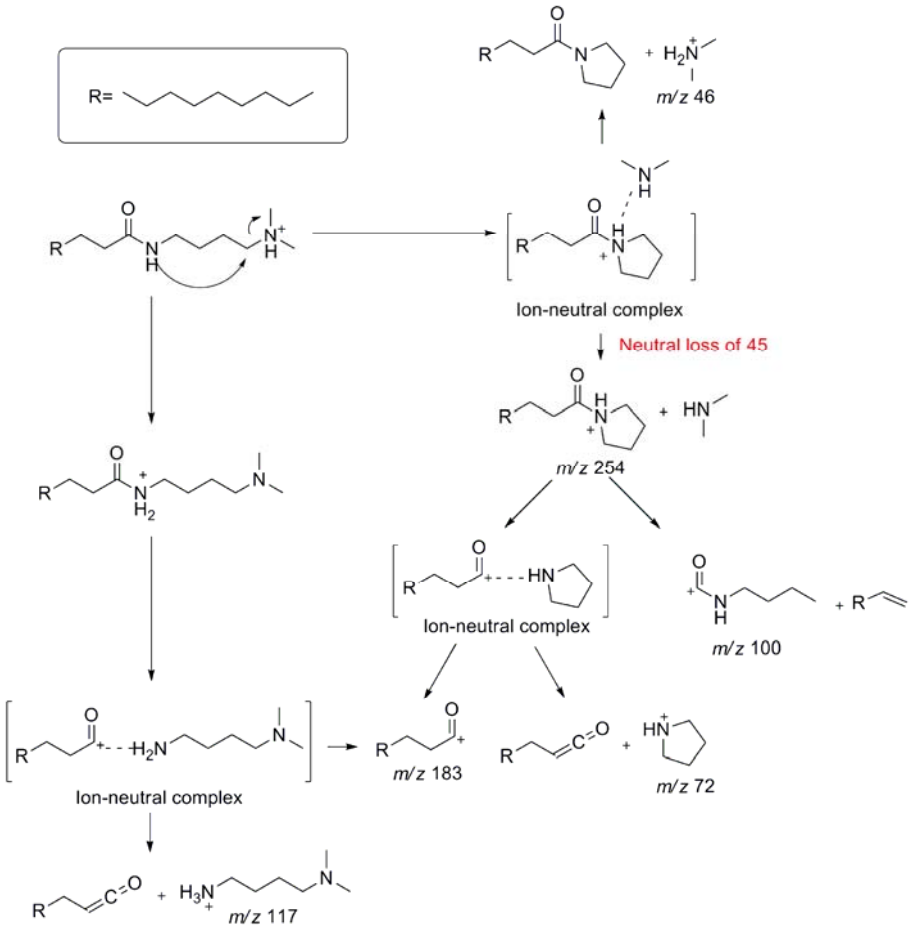

**Figure 5** Volcano plot demonstrating differences in metabolite contents between wounded and non-wounded tomato leaves. The plot reveals a small proportion of metabolites that meet our arbitrary criteria. Horizontal line, $p$ = 0.01; vertical lines, 1.50-fold changes (|$\log_2$ fold change|=0.585), both up- and down-regulated.

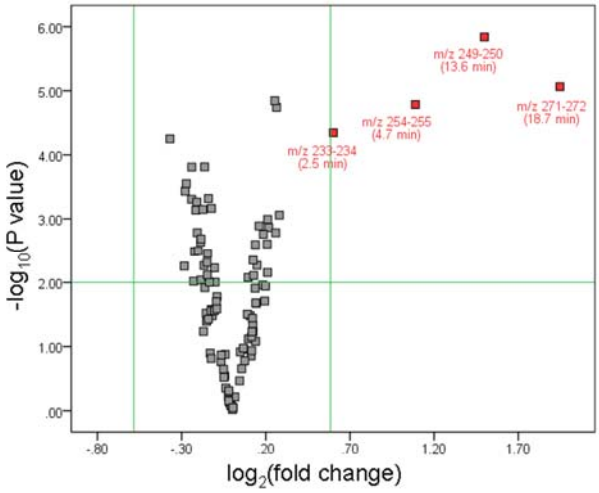

**Figure 6** The integrative plot of the potential biomarkers of wounded tomato leaves.

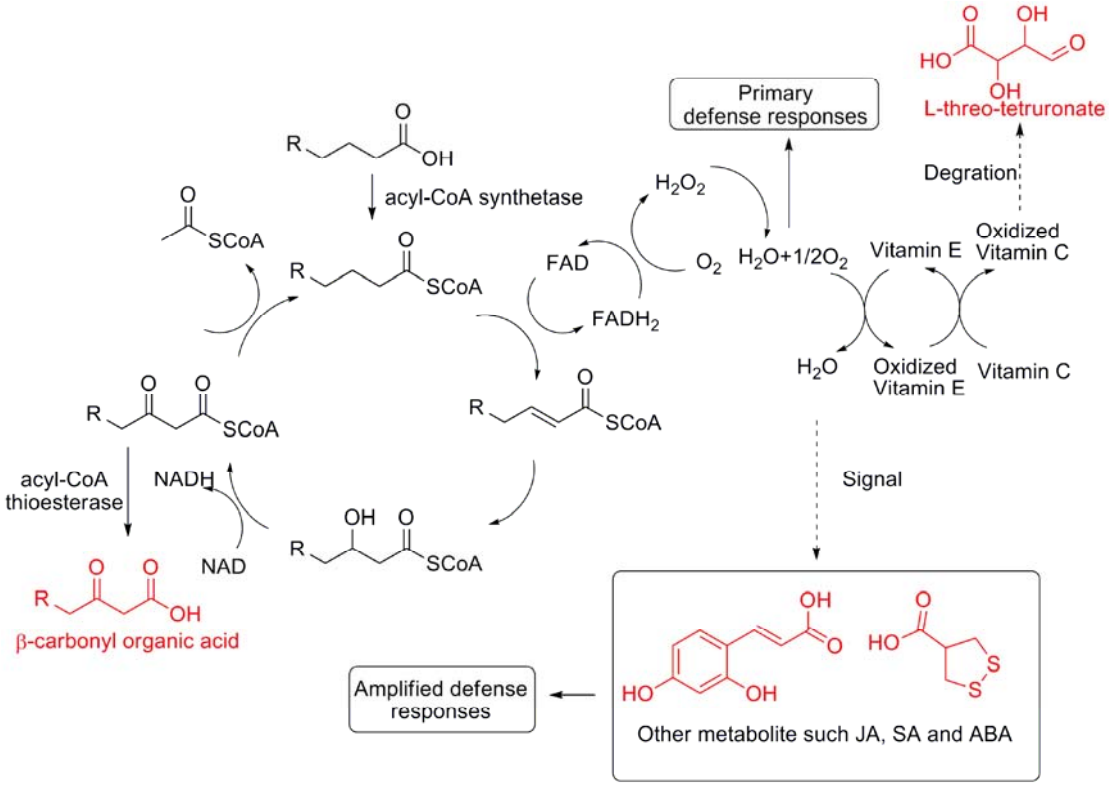

**Figure 7** Comparison of neutral loss scan and full scan mode. Full scan mass spectrum (A) and neutral loss scan mass spectrum (B) at the retention time of 3-oxo-nonanoic acid (18.6-19.2 min, *m/z* 271).

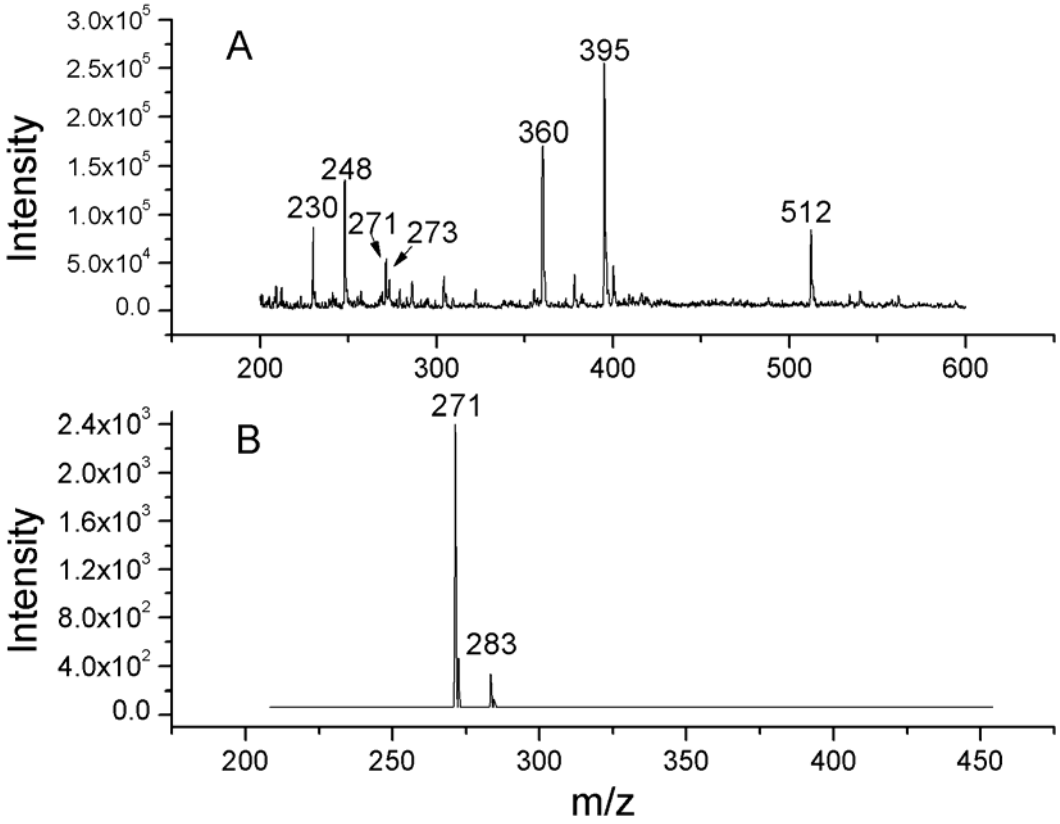

## Graphical Abstract

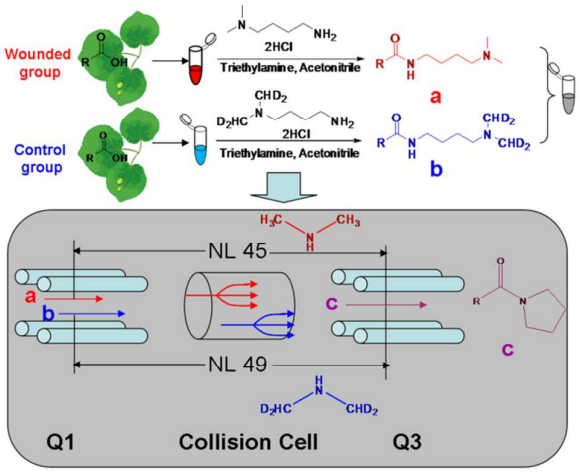


The development of a method for non-targeted screening of metabolites with carboxyl group by high performance liquid chromatography-mass spectrometry with paired homologous double neutral loss scan mode after in vitro isotope labelling was reported.